

# Remarkable Improvement of Creep Strength by Vanadium Addition in 2.25Cr Heat-Resistant Steel

Hyun Je SUNG<sup>1)</sup> and Sung-Joon KIM<sup>2)\*</sup>

1) Technical Research Laboratories, POSCO, Pohang, 37859 South Korea. 2) Graduate Institute of Ferrous Technology, Pohang University of Science and Technology (POSTECH), Pohang, 37673 South Korea.

(Received on April 11, 2018; accepted on July 12, 2018)

This paper reports the effect of vanadium (V) addition on elimination of easily coarsening  $M_{23}C_6$  carbide and on remarkable creep strength improvement in T/P23 heat-resistant steel (2.25Cr-1.5W-VNbTi). Increase in V content eliminates coarse  $M_{23}C_6$  and allows only precipitation of MX carbo-nitrides in T/P23 heat-resistant steel. Fine MX effectively stabilizes sub-boundaries of bainite microstructure, so coalescence of neighboring sub-boundaries and subsequent creep strength loss are suppressed. This steel even surpasses the creep life of conventional 9 wt.% Cr steels due to powerful sub-boundary hardening.

KEY WORDS: precipitation; MX carbo-nitride; sub-boundary; creep; heat-resistant steels.

## 1. Introduction

Creep strength of heat-resistant steels can be increased by precipitation of finely-dispersed MX carbo-nitrides (M = metallic element such as V, Nb, Ti; X = C or N).<sup>1)</sup> This concept has been applied to T/P22 (2.25Cr-1Mo), then T/P24 (2.25Cr-1Mo-VNbTi) heat-resistant steel was introduced.<sup>2)</sup> T/P23 heat-resistant steel (2.25Cr-1.5W-VNbTi) was developed by alloying W instead of Mo in T/P24. W increases solid solution strengthening, as a result of the difference in atomic radii between W and Fe. MX carbo-nitrides that contain W can keep good coherency with the matrix and increase the shear stress for dislocation even after long exposure to high temperature.<sup>3)</sup> The creep strength of T/P23 steel is higher than that of T/P24 steel and similar to that of T/P91 steel (9Cr-1Mo-VNbTi). Consequently, T/P23 steel has been widely used for water-wall panels of ultra-supercritical boilers.

Increase in steam temperature and pressure in turbine significantly improves efficiency of power plant; this influences the operating conditions of water-walls. Therefore, new heat-resistant steels need to be developed for the requirements of advanced boilers such as higher steam temperature and pressure. Also, low-Cr heat-resistant steels have been required to be developed for replacing high-Cr-containing steels in order to construct power plant at a reasonable budget.

The minimum creep rate of 9Cr-3W-3Co-0.2V-0.05Nb-0.05N martensitic heat-resistant steel at 650°C under 140 MPa was reduced by decreasing the C content from 0.078 wt.% to extremely low 0.002 wt.%.<sup>4-6)</sup> Unstable and easily-coarsened  $M_{23}C_6$  carbide is not formed completely,

and the fine MX carbo-nitrides prohibit dislocation movement toward lath boundaries and block boundaries, so dislocation annihilation can be suppressed. Hence, the onset of acceleration creep is delayed. Consequently, elimination of  $M_{23}C_6$  carbides and dispersion of MX carbo-nitrides are the keys to creep strengthening. Here, increase in V content can be a good solution for creep life extension of T/P23. In the former case, bulk V content ( $[V]$ ) > 0.4 wt.% inhibits the precipitation of  $M_{23}C_6$  carbide in T/P23 heat-resistant steel at 750°C.<sup>7)</sup> In the latter case, fine V-rich MX precipitation can be controlled by austenitization and tempering; it is much easier than precipitation of Ti-rich MX which is extremely stable up to melting temperature of steel.

Therefore, this research quantifies how creep strength of T/P23 steel is affected by  $[V]$  > 0.4 wt.%, which can avoid the difficult process of obtaining extremely-low-C alloy.

## 2. Experimental Procedure

Three T/P23 steel ingots with  $[V]$  = 0.255 wt.% (V255), 0.620 wt.% (V620) and 0.798 wt.% (V798) were prepared by vacuum induction melting; their chemical compositions (**Table 1**) were measured using an optical emission spectrometer (OES, OBLF QSN-750) and a carbon/sulfur analyzer (LECO CS-844). The ingots were homogenized at 1 200°C for 1 h and hot-rolled to 12 mm thick plates. Rectangular bars with a dimension of 12 × 12 × 130 mm were machined from the plates in the hot-rolling direction. These bars were given to heat treatment (austenitization at 1 050°C for 1 h followed by air cooling and subsequent tempering at 750°C for 0.5 h under Ar atmosphere).

Cylindrical specimens (gauge length 25 mm, gauge diameter 6.25 mm) were machined from the bars, then used to assess their creep strength at 600°C without soaking in ambient condition, using conventional creep testers

\* Corresponding author: E-mail: sjkim1@postech.ac.kr  
DOI: <https://doi.org/10.2355/isijinternational.ISIJINT-2018-265>

**Table 1.** Chemical compositions of the prepared steels (wt.%).

	C	Si	Mn	P	S	Cr	Mo	V	Al	W	Nb	N	B	Ti	Fe
V255	0.100	0.318	0.509	0.021	<0.002	2.24	0.05	0.255	0.019	1.55	0.049	0.010	0.0013	0.016	Bal.
V620	0.103	0.317	0.534	0.020	<0.002	2.24	0.03	0.620	0.023	1.51	0.049	0.010	0.0008	0.011	Bal.
V798	0.098	0.318	0.512	0.019	<0.002	2.26	0.03	0.798	0.017	1.54	0.049	0.013	0.0009	0.010	Bal.

(ATS 2320). The microstructure was investigated using a field-emission scanning electron microscope (FE-SEM, ZEISS ULTRA-55) at 10 kV. Precipitates in the carbon extraction replica and in the thin foil specimens were analyzed using a field-emission transmission electron microscope (FE-TEM, JEOL JEM-2100F) equipped with an energy-dispersive spectroscope (EDS, OXFORD) at 200 kV.

### 3. Results and Discussion

The Gibbs free energy difference for  $M_{23}C_6$  carbide formation becomes positive when  $[V] > 0.4$  wt.% at the temperatures of tempering ( $750^\circ\text{C}$ )<sup>7</sup> and of the creep test ( $600^\circ\text{C}$ ) (Fig. 1); this change would discourage the formation of  $M_{23}C_6$  carbide in V620 and V798. Consistent with this prediction, it is confirmed by SEM and TEM that V255 has large Cr-rich  $M_{23}C_6$  carbides  $\sim 250$  nm size on boundaries, together with MX carbo-nitrides (Figs. 2 and 3), whereas V620 and V798 both contain only fine MX carbo-nitrides  $< 20$  nm size along boundaries and in the matrix (Figs. 4 and 5) after the heat treatment. In particular, V-rich MX carbo-nitrides are mainly found and W also participates in formation of carbo-nitrides. All specimens contained tempered bainite microstructure and had similar narrow plate-like bainite sub-grains.<sup>8</sup>) Also, all steels showed similar mean short width of plate-like sub-grains ( $\lambda_{sg}$ )  $\sim 0.55$   $\mu\text{m}$ .

The amount of V-rich MX carbo-nitrides at tempering temperature of  $750^\circ\text{C}$  (Fig. 6(a)) and creep test temperature of  $600^\circ\text{C}$  (Fig. 6(b)) increased significantly as  $[V]$  increased from 0.255 wt.% to 0.620 wt.%, but not with further increase to 0.798 wt.%.  $M_6C$  carbide rich in Fe and W is also one of the equilibrium precipitates, but it was not found after the tempering at  $600^\circ\text{C}$ . However,  $M_6C$  can form after long-term aging<sup>3,9</sup>) and its volume fraction is expected to be similar among V255, V620 and V798 at the creep test temperature of  $600^\circ\text{C}$  (Fig. 6(b)). The amount of Nb- and Ti-rich carbo-nitrides decreased as  $[V]$  increased, but this change is very insignificant, compared with V-rich MX.

Creep lives of V255 were similar to those of T/P23 and T/P91 heat-resistant steels examined by National Institute for Materials Science (NIMS), Japan (Fig. 7(a)).<sup>10</sup>) As  $[V]$  was increased from 0.255 to 0.620 wt.%, time to failure remarkably increased, but V620 and V798 showed similar creep lives. Both V620 and V798 are stronger than T/P92 steel (9Cr-1.8W-0.5Mo-VNbTi), based on NIMS data.<sup>10</sup>) The V255 ruptured at 6 427 h under 125 MPa at  $600^\circ\text{C}$ , whereas the V798 has endured applied stress for  $\sim 12$  000 h with very low creep deformation; this test is ongoing (Fig. 7(b)).

Addition of  $[V]$  greater than ASTM A213 standard range<sup>1,2</sup>) causes precipitation hardening and sub-boundary

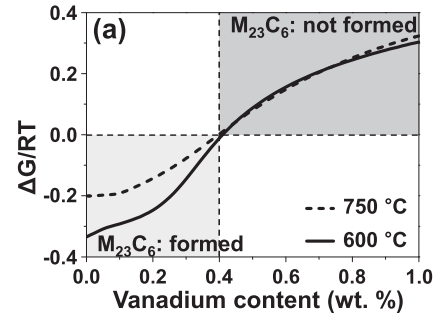


**Fig. 1.** Changes in Gibbs free energy difference of  $M_{23}C_6$  formation with bulk vanadium content (calculated by Thermo-Calc with TCFE7 database).

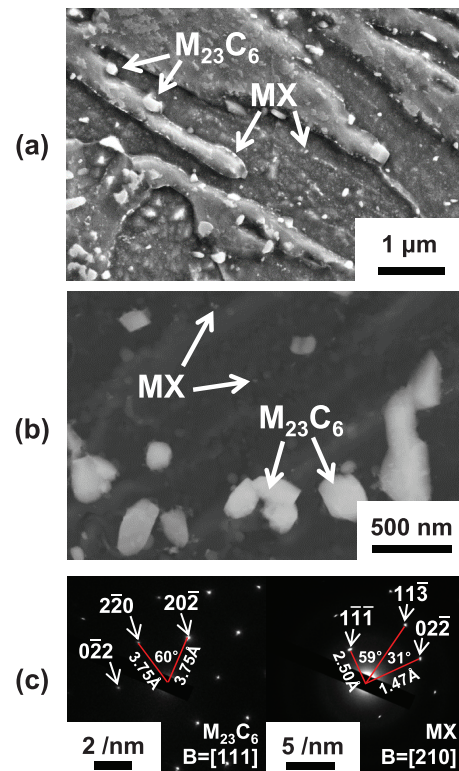


**Fig. 2.** Micrographs of V255 after heat treatment (normalization at  $1\ 050^\circ\text{C}$ , subsequent tempering at  $750^\circ\text{C}$ ): (a) scanning electron micrograph, (b) scanning transmission electron microscopy-dark field (STEM-DF) image and (c) diffraction patterns (DPs) of  $M_{23}C_6$  carbide and MX carbo-nitride. (b) and (c) are images of precipitates on carbon extraction replica. (Online version in color.)

hardening, both of which increase creep strength. Firstly, increase in density of the distribution of V-rich MX significantly decreases interparticle spacing. The stress required to pass precipitates (Orowan stress) is given by

$$\sigma_{\text{or}} = 0.8MGb / \lambda_p$$

where  $M$  is the Taylor factor,<sup>11</sup>)  $G$  is the shear modulus,<sup>10,12</sup>)

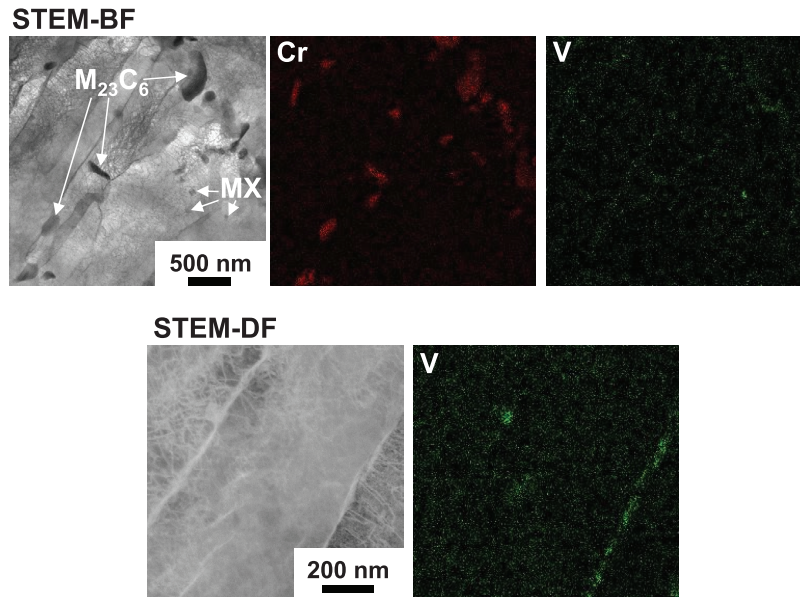


**Fig. 3.** STEM-bright field (STEM-BF) image, STEM-DF image and EDS mapping images in thin foil V255 specimen after heat treatment (normalization at 1 050°C, subsequent tempering at 750°C). (Online version in color.)

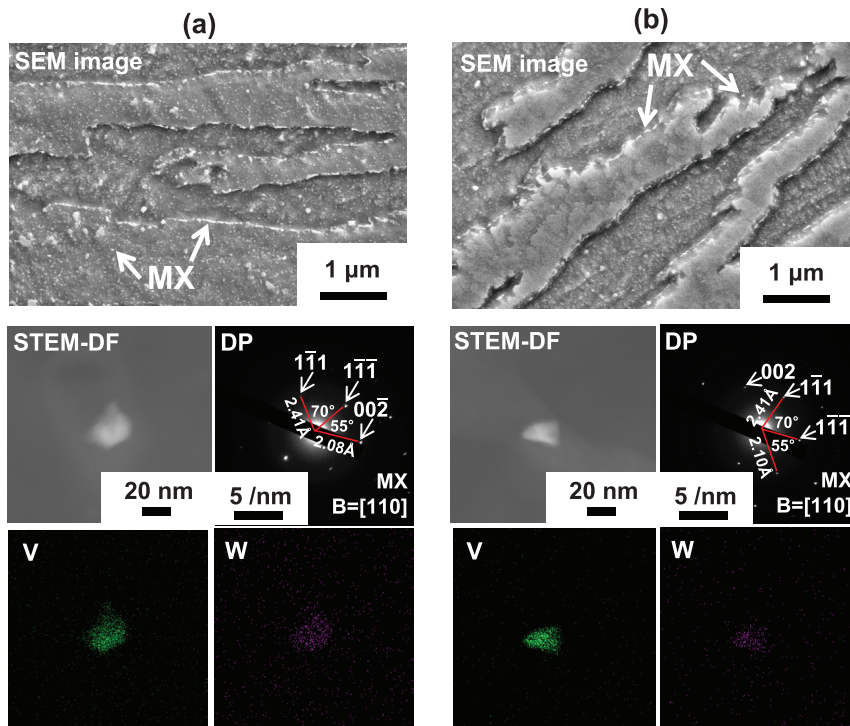


**Fig. 4.** Scanning electron micrographs, STEM-DF images, DPs and EDS mapping images of MX carbo-nitrides on carbon extraction replica of (a) V620 and (b) V798 after heat treatment (normalization at 1 050°C, subsequent tempering at 750°C). (Online version in color.)

$b$  is the Burgers vector<sup>11)</sup> and  $\lambda_p$  is the mean particle spacing confirmed by TEM (Figs. 3 and 5). Orowan stress is increased with decreasing  $\lambda_p$  (Table 2). Therefore, dislocation annihilation can be suppressed, as a result of prohibited dislocation movement toward lath boundaries and block boundaries. Furthermore, sub-grain microstructure in bainite can provide a hardening effect at high temperature.<sup>13,14)</sup> The sub-boundary hardening is given by

$$\sigma_{sg} = 10Gb / \lambda_{sg}$$

where  $\lambda_{sg}$  is the mean short width of plate-like sub-grains

confirmed by SEM and TEM (Figs. 2, 3, 4 and 5),  $\sim 0.55 \mu\text{m}$  in this research. The influence of this phenomenon is higher than the Orowan stress from  $\text{M}_{23}\text{C}_6$  and MX (Table 3), so sub-boundary hardening can be regarded as a main strengthening mechanism. However, sub-grain can be finally coarsened by progressive local coalescence of adjoined sub-grain boundaries forming Y-junction, or of neighboring boundaries under applied stress at high temperature.<sup>14,16,17)</sup>  $\text{M}_{23}\text{C}_6$  in the V255 easily coarsens during creep,<sup>3,9,13,14)</sup> so it cannot stabilize the sub-grain boundaries. Moving sub-boundaries coalesce with each other (Fig. 8(a))

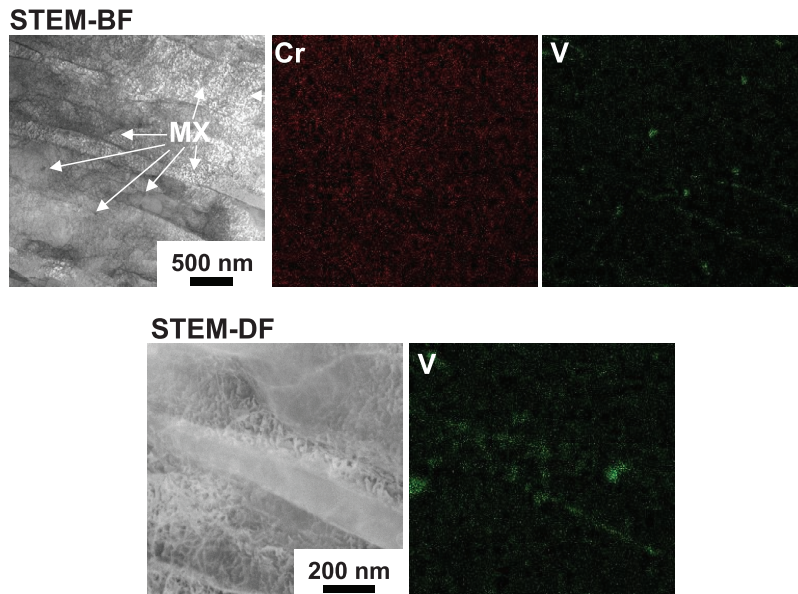


Fig. 5. STEM-BF image, STEM-DF image and EDS mapping images in thin foil V798 specimen after heat treatment (normalization at 1 050°C, subsequent tempering at 750°C). (Online version in color.)

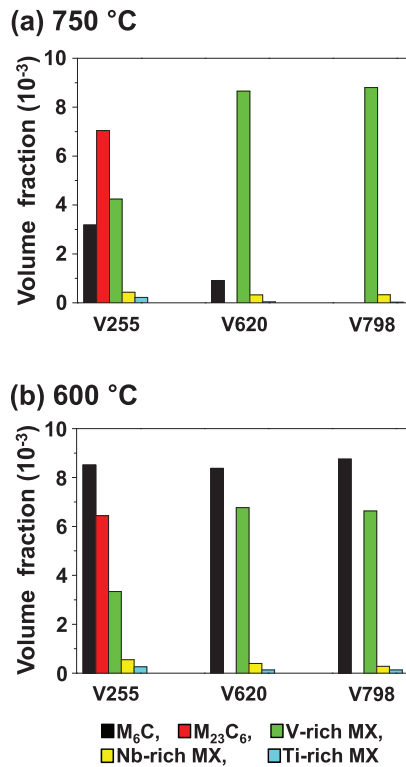


Fig. 6. (a) Volume fraction of equilibrium precipitates at tempering temperature of 750°C and (b) at creep test temperature of 600°C calculated by Thermo-Calc with TCFE7 database. (Online version in color.)

Table 2. Calculation result of precipitation hardening effect  $\sigma_{or}$ .  $M$ : Taylor factor,<sup>11)</sup>  $G$ : shear modulus,<sup>10,12)</sup>  $b$ : Burgers vector,<sup>11)</sup>  $\lambda_p$ : mean particle spacing.

Equation	$M$	$G$ (GPa)	$b$ (nm)	$\lambda_p$ (nm)	$\sigma_{or}$ (MPa)
$\sigma_{or} = 0.8MGb/\lambda_p$	3	63.26	0.25	M <sub>23</sub> C <sub>6</sub> : 260 (V255)	146
				MX: 230 (V255)	165
				MX: 140 (V620&V798)	271

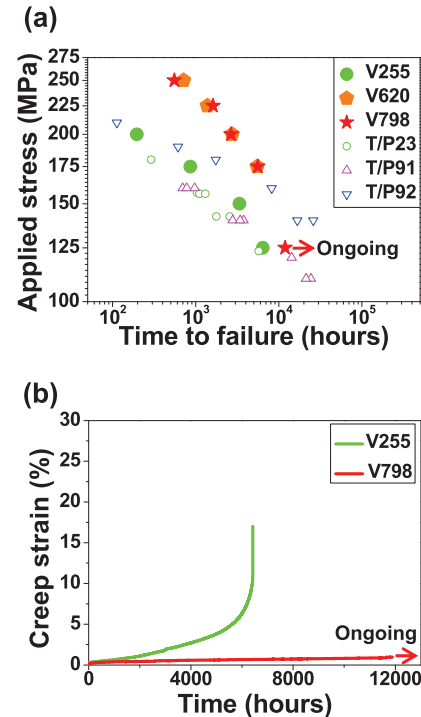


Fig. 7. (a) Creep test results of V255, V620 and V798 together with ASTM T/P23, T/P91 and T/P92 steels performed by National Institute for Materials Science (NIMS), Japan, (b) measured creep strain under 125 MPa at 600°C. (Online version in color.)

Table 3. Calculation result of sub-boundary hardening effect  $\sigma_{sg}$ .<sup>13,14)</sup>  $\lambda_{sg}$ : mean short width of plate-like sub-grains.

Equation	$G$ (GPa)	$b$ (nm)	$\lambda_{sg}$ ( $\mu$ m)	$\sigma_{sg}$ (MPa)
$\sigma_{sg} = 10Gb/\lambda_{sg}$	63.26	0.25	0.55	288

and migration of sub-boundaries can absorb dislocations in the matrix; recovery, increase in short width of plate-like sub-grains, and creep strength loss occur. In contrast, the initial microstructures of V620 and V798 show only fine and dense MX distribution, mainly V-rich carbo-nitrides.

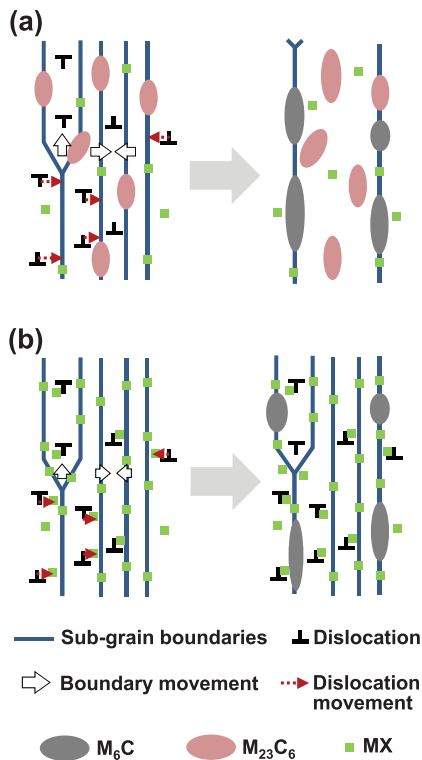


Fig. 8. Schematic illustration of creep behavior of (a) V255, (b) V620 and V798. (Online version in color.)

Dislocations in low-angle sub-boundary walls can be stabilized by finely-distributed carbo-nitrides (Fig. 8(b)),<sup>13–15</sup> so sub-grain coarsening can be effectively prohibited. Owing to powerful sub-boundary hardening from MX carbo-nitrides, V620 and V798 have higher creep strength than 9 wt.% Cr T/P92 heat-resistant steel, which has unstable  $M_{23}C_6$  carbides<sup>18</sup>) (Fig. 7(a)). Considering that the volume fractions of  $M_6C$  carbide are similar at creep test temperature of 600°C regardless of [V] (Fig. 6(b)), the difference in precipitation reactions of  $M_{23}C_6$  and V-rich MX might be the main factor that controls creep strength.

W-alloying to the MX effectively decreases growth rate of carbo-nitrides,<sup>3)</sup> so fine distribution of (V, W) X can mainly stabilize bainite sub-structure. TEM-EDS analysis detected a very tiny difference of W-alloying to carbo-nitrides between V620 and V798 after the tempering at 750°C (Fig. 9(a)); this similarity is the reason that both specimens show similar sizes of carbo-nitrides (Fig. 4). Therefore, together with the similar amount of V-rich MX in both steels (Fig. 6), this similarity in sizes of carbo-nitrides leads to similar creep lives (Fig. 7(a)). However, alloying of W in the equilibrium (V, W)X is expected to be higher in V620 at 600°C (Fig. 9(b)), based on calculation results performed by Thermo-Calc with TCFE7 database. Hence, further research should investigate the effect of [V] on changes in W-alloying in MX, on MX size, on sub-boundary hardening and on creep strength at high temperature.

#### 4. Summary

Creep strength of T/P23 heat-resistant steel was significantly increased by addition of [V] > 0.4 wt.%. The easily coarsened  $M_{23}C_6$  does not precipitate, but nano-sized MX carbo-nitrides dominantly precipitate in steel that

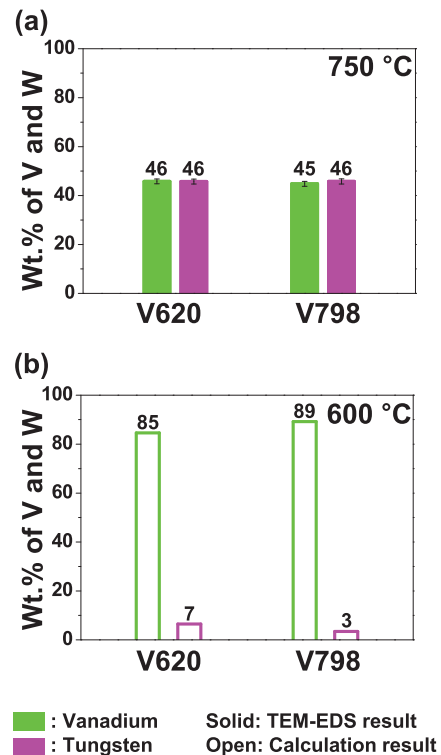


Fig. 9. (a) TEM-EDS results showing weight percentage of tungsten and vanadium in metallic elements of MX after tempering at 750°C and (b) calculation results performed by Thermo-Calc with TCFE7 database at creep test temperature 600°C. (Online version in color.)

has [V] > 0.4 wt.%. Nano-sized MX carbo-nitrides on sub-boundaries can stabilize dislocations in low-angle sub-boundary walls and obstruct the coalescence of neighboring sub-boundaries; this stabilization helps sub-boundary hardening to persist during creep. Finely-dispersed MX also increases creep strength by increasing precipitation hardening. Consequently, this research suggests a new alloy design for low-Cr heat-resistant steel that has higher creep strength than conventional 9 wt.% Cr steels.

#### REFERENCES

- W. Bendic, J. Gabrel, B. Hahn and B. Vandenberghe: *Int. J. Press. Vessel. Pip.*, **84** (2007), 13.
- J. C. Vaillant, B. Vandenberghe, B. Hahn, H. Heuser and C. Jochum: *Int. J. Press. Vessel. Pip.*, **85** (2008), 38.
- K. Miyata and Y. Sawaragi: *ISIJ Int.*, **41** (2001), 281.
- M. Taneike, F. Abe and K. Sawada: *Nature*, **424** (2003), 294.
- M. Taneike, K. Sawada and F. Abe: *Metall. Mater. Trans. A*, **35** (2004), 1255.
- F. Abe, T. Horiuchi, M. Taneike and K. Sawada: *Mater. Sci. Eng. A*, **378** (2004), 229.
- H. J. Sung, N. H. Heo and S.-J. Kim: *Metall. Mater. Trans. A*, **48** (2017), 1459.
- B. Josefsson and H.-O. Andrén: *J. Phys. Colloq.*, **49** (1988), C6-293.
- K. Miyata, M. Igarashi and Y. Sawaragi: *ISIJ Int.*, **39** (1998), 947.
- NIMS: Creep Data Sheet, MatNavi NIMS Materials Database, [http://smds.nims.go.jp/creep/index\\_en.html](http://smds.nims.go.jp/creep/index_en.html), (accessed 2017-08-03).
- F. Abe: *Sci. Technol. Adv. Mater.*, **9** (2008), 1.
- K. M. Zwilsky: ASM Handbook, Properties and Selection: Irons, Steels and High Performance Alloys, Vol. 1, 10th ed., ASM International, Materials Park, (1993), 1452.
- K. Maruyama, K. Sawada and J. Koike: *ISIJ Int.*, **41** (2001), 641.
- F. Abe: *Mater. Sci. Eng. A*, **387** (2004), 565.
- F. Abe, M. Taneike and K. Sawada: *Int. J. Press. Vessel. Pip.*, **84** (2007), 3.
- J. J. Gilman: *Acta Metall.*, **3** (1955), 277.
- J. C. M. Li: *Acta Metall.*, **8** (1960), 563.
- H. J. Sung, N. H. Heo and S.-J. Kim: *ISIJ Int.*, **57** (2017), 1268.